New Phytologist

# A tonoplast-localized magnesium transporter is crucial for stomatal opening in Arabidopsis under high $Mg^{2+}$ conditions

Shin-ichiro Inoue[1] (iD), Maki Hayashi[1] (iD), Sheng Huang[2] (iD), Kengo Yokosho[2] (iD), Eiji Gotoh[3] (iD), Shuka Ikematsu[4] (iD), Masaki Okumura[1], Takamasa Suzuki[5] (iD), Takumi Kamura[1], Toshinori Kinoshita[1,4] (iD) and Jian Feng Ma[2] (iD)

[1]Division of Biological Science, Graduate School of Science, Nagoya University, Furo-cho, Chikusa-ku, Nagoya, Aichi 464-8602, Japan; [2]Institute of Plant Science and Resources, Okayama University, Chuo 2-20-1, Kurashiki 710-0046, Japan; [3]Department of Forest Environmental Sciences, Faculty of Agriculture, Kyushu University, 744 Motooka, Fukuoka 819-0395, Japan; [4]Institute of Transformative Bio-Molecules (WPI-ITbM), Nagoya University, Furo-cho, Chikusa, Nagoya 464-8602, Japan; [5]Department of Biological Chemistry, College of Bioscience and Biotechnology, Chubu University, Kasugai-shi, Aichi 487-8501, Japan

Authors for correspondence:
*Shin-ichiro Inoue*
*Email: shin@bio.nagoya-u.ac.jp*

*Toshinori Kinoshita*
*Email: kinoshita@bio.nagoya-u.ac.jp*

*Jian Feng Ma*
*Email: maj@rib.okayama-u.ac.jp*

## Summary

- Plant stomata play an important role in $CO_2$ uptake for photosynthesis and transpiration, but the mechanisms underlying stomatal opening and closing under changing environmental conditions are still not completely understood.
- Through large-scale genetic screening, we isolated an Arabidopsis mutant (*closed stomata2* (*cst2*)) that is defective in stomatal opening. We cloned the causal gene (*MGR1/CST2*) and functionally characterized this gene.
- The mutant phenotype was caused by a mutation in a gene encoding an unknown protein with similarities to the human magnesium ($Mg^{2+}$) efflux transporter ACDP/CNNM. MGR1/CST2 was localized to the tonoplast and showed transport activity for $Mg^{2+}$. This protein was constitutively and highly expressed in guard cells. Knockout of this gene resulted in stomatal closing, decreased photosynthesis and growth retardation, especially under high $Mg^{2+}$ conditions, while overexpression of this gene increased stomatal opening and tolerance to high $Mg^{2+}$ concentrations. Furthermore, guard cell-specific expression of *MGR1/CST2* in the mutant partially restored its stomatal opening.
- Our results indicate that MGR1/CST2 expression in the leaf guard cells plays an important role in maintaining cytosolic $Mg^{2+}$ concentrations through sequestering $Mg^{2+}$ into vacuoles, which is required for stomatal opening, especially under high $Mg^{2+}$ conditions.

## Introduction

Stomatal pores, formed by pairs of guard cells in the plant epidermis, regulate gas exchange between plants and the atmosphere. Stomatal opening is required for $CO_2$ uptake for photosynthesis and water transpiration for maintaining leaf temperature (Roelfsema & Hedrich, 2005; Shimazaki *et al.*, 2007). A number of studies have investigated the mechanisms of stomatal opening and closing in different plant species, especially in Arabidopsis. Among them, light has been shown to be a key environmental cue which induces stomatal opening under natural conditions. The stomatal responses to light are regulated by two distinct light-activated signaling pathways: a blue light pathway and a photosynthetically active radiation (PAR)-dependent pathway (Willmer & Fricker, 1996; Shimazaki *et al.*, 2007; Matthews *et al.*, 2020). Blue light acts directly on guard cells to induce stomatal signaling, while PAR acts both directly and indirectly on guard cells. It has been suggested that guard cell photosynthesis generates ATP and/or reducing equivalents for stomatal opening (Tominaga *et al.*, 2001; Suetsugu *et al.*, 2014; Santelia & Lawson, 2016), and mesophyll cell photosynthesis induces a decrease in $CO_2$ in the leaves, which acts on guard cells to mediate the opening of stomata (Assmann, 1988; Shimazaki *et al.*, 2007; Suetsugu *et al.*, 2014).

Stomatal opening is driven by the swelling of guard cells in response to blue light, suggesting that a single guard cell possesses all signaling components, from blue light-perception to a mechanism for increasing cell volume, for stomatal opening (Zeiger & Hepler, 1977; Shimazaki *et al.*, 2007). Blue light activates the plasma membrane $H^+$-ATPase via photoreceptor phototropin-mediated signaling (Kinoshita *et al.*, 2001; Inoue *et al.*, 2008). The activated $H^+$-ATPase hyperpolarizes the plasma membrane, followed by activation of inward-rectifying $K^+$ channels (Schroeder *et al.*, 2001; Lebaudy *et al.*, 2008; Marten *et al.*, 2010). In

addition, phototropin signaling distinct from the $H^+$-ATPase pathway activates the $K^+$ channels via CBL-interacting protein kinase 23 (CIPK 23) (Zhao et al., 2012; Inoue et al., 2020). This $K^+$ channel activation induces an influx of $K^+$, resulting in the accumulation of $K^+$ and the counter anions of $Cl^-$, nitrate ($NO^{3-}$) (Guo et al., 2003) and malate$^{2-}$ in guard cells. The $K^+$ and $Cl^-$ ions are transported into the vacuole via the tonoplast-localized transporters $Na^+/H^+$ exchanger (NHX)1 and NHX2, the detoxification efflux carriers (DTX)33 and DTX35, and the channels Aluminum-activated Malate Transporter (ALMT)9 and Chloride Channel C (CLC-c), respectively (Jossier et al., 2010; De Angeli et al., 2013; Andrés et al., 2014; Zhang et al., 2017). Malate$^{2-}$ is also transported into the vacuole via ALMT6 and 9 (Eisenach & De Angeli, 2017). Accumulation of these ions decreases the guard-cell water potential, leading to water uptake into the vacuole and turgor increase, which finally induces stomatal opening (Inoue et al., 2010; Marten et al., 2010). Thus, the vacuolar volume increase by ion and water uptake is crucial for stomatal opening (Eisenach & De Angeli, 2017; Martinoia, 2018). Apart from these ion transport events, starch degradation in guard cell chloroplasts is induced downstream of phototropin-activated $H^+$-ATPase, which also contributes to stomatal opening without affecting the capacity of guard-cell ion transport (Horrer et al., 2016; Flütsch et al., 2020). However, these signaling mechanisms and the regulatory mechanisms for each event have not been fully elucidated, and our understanding of stomatal opening is still not sufficient, especially under changing environments.

In this study, to identify novel factors involved in stomatal opening, we performed a large-scale screening of mutants defective in stomatal opening in Arabidopsis using infrared thermography. Through gene mapping and detailed functional analysis of one mutant (cst2 for closed stomata 2), we found that MGR1/CST2, a tonoplast-localized $Mg^{2+}$ transporter, is involved in stomatal opening through sequestering $Mg^{2+}$ into the vacuole to maintain cytosolic $Mg^{2+}$ concentration in the guard cells in Arabidopsis, especially under high $Mg^{2+}$ conditions.

## Materials and Methods

### Plant materials and growth conditions

Arabidopsis thaliana (L.) Heynh Col-0 was used as a wild-type (WT). T-DNA insertion mutants (Col-0 background), and cst2-2 (GABI_322H07) were obtained from the Nottingham Arabidopsis Stock Centre (NASC). All lines, including cst2-1, that were used for growth and stomatal aperture measurements were grown on soil or nutrient solution with a 14 h : 10 h, light : dark photoperiod under white fluorescent light (50 µmol m$^{-2}$ s$^{-1}$) at 22–24°C. Nicotiana benthamiana used for transient expression of fluorescent proteins was grown under similar conditions to the Arabidopsis plants.

Hydroponic cultivation was performed using the Araponics Growing System (Araponics, Liège, Belgium). Plants were grown on ½ Murashige & Skoog (½MS) agar medium for 7 d, and then transferred to a nutrient solution (Norén et al., 2004). The solution was constantly aerated and replaced every 4 d.

For agar medium growth, plants were grown on ½MS agar medium (0.8% (w/v) agar, 0.05% (w/v) MES, pH 5.8), with or without $MgSO_4$ supplementation, at various concentrations. The ½MS medium contained 0.75 mM $Mg^{2+}$.

### Screening of mutants defective in stomatal opening

Ethyl methanesulfonate-mutagenized M2 seeds purchased from Lehle Seeds (the trichome-less glabra1 background), were used for screening of mutants as described previously (Inoue et al., 2017). Plants were grown in soil for 3 wk. At 21–25 d, leaf temperature was measured using an infrared thermograph (TVS-500EX; NEC Avio Infrared Technology, Yokohama, Japan). Thermal images were analyzed using the AVIO THERMOGRAPHY STUDIO software package (NEC Avio Infrared Technology).

### Gene mapping

To map the gene responsible for the cst2 phenotype, the homozygous cst2-1 mutant in the Col accession background was crossed with the Ler accession to generate a mapping population. Based on growth retardation of F2 seedlings grown in soil and polymorphism markers distributed throughout the five Arabidopsis chromosomes, the responsible gene was mapped to chromosome 4. To further identify the responsible mutation, genomic DNA was extracted from the bulked seedlings showing mutant and WT phenotypes and used for library construction for sequencing. A total of 1.99 Gbp, c. 17 times the size of the Arabidopsis genome, was sequenced, and the short reads obtained were analyzed and compared by the MITSUCAL computer system (Suzuki et al., 2018) to identify the cst2 mutation.

### Construction of phylogenetic tree

Amino acid sequences of MGR1/CST2 homologs were aligned using MUSCLE (Edgar, 2004). The phylogenetic tree was constructed using the neighbor-joining method and bootstrapping with 1000 replications in MEGAX (Kumar et al., 2018). Full-length amino acid sequences of MGR1/CST2 and homolog proteins were used to construct phylogenetic tree.

### Measurement of magnesium concentrations in plants

For comparisons of Mg concentrations, seedlings of WT and cst2 mutants were grown on ½MS agar medium with or without 5 mM $MgSO_4$ for 3 wk. The shoots were harvested and washed with Milli Q water four times and dried at 70°C for at least 3 d. The dried samples were digested with concentrated $HNO_3$ (60%) at 140°C. The concentration of Mg in the digest solution was determined using inductively coupled plasma mass spectrometry (ICP-MS) (7700X; Agilent Technologies, Santa Clara, CA, USA) as described previously (Yamaji et al., 2017).

## Measurement of stomatal aperture and stomatal conductance

The (4-wk-old) seedlings grown in soil or hydroponically were kept in the dark before measurement. Rosette leaves were harvested from the dark-adapted plants, and epidermal fragments were isolated using a blender (Waring Commercial, Stamford, CT, USA) under dim red light. The epidermal fragments were collected on a 58 μm nylon mesh and used for stomatal aperture measurement according to the method described by Inoue *et al.* (2008) and de Carbonnel *et al.* (2010), with minor modifications. Briefly, to determine the effect of $Mg^{2+}$ on stomatal opening, the epidermal fragments were incubated in 2 ml KCl-based buffer (5 mM MES/bistrispropane (pH 6.5), 50 mM KCl, and 0.1 mM $CaCl_2$) as a positive control, the $MgCl_2$-based buffer (5 mM MES/bistrispropane (pH 6.5), 25 mM $MgCl_2$, and 0.1 mM $CaCl_2$), or the KCl/$MgCl_2$-based buffer (5 mM MES/bistrispropane (pH 6.5), 25 mM KCl, 12.5 mM $MgCl_2$, and 0.1 mM $CaCl_2$). After illumination with light for 3 h at room temperature, the stomatal apertures were measured at the abaxial epidermis under a microscope, by focusing on the inner lips of stomata.

Stomatal conductance in intact leaves of WT and *cst2* mutants was determined according to the methods described by Doi *et al.* (2004) and Gotoh *et al.* (2019). The hydroponically grown plants were used for measurement.

## Transport activity assay of MGR1/CST2 in yeast

To determine the transport activity of MGR1/CST2 for $Mg^{2+}$, the yeast mutant *mam3* was used. Yeast strain BY4741 (as the WT) and the *mam3* mutant (4741, *mam3 Δ:: KANR*) were purchased (Thermo Fisher Scientific, Waltham, MA, USA). The *MAM3* coding sequence and *MGR1/CST2* cDNA were amplified from the yeast genome and Arabidopsis cDNA, respectively, using the primers MAM3_F and MAM3_R for *MAM3*, and MGR1/CST2_F and MGR1/CST2_R for *MGR1/CST2* (Supporting Information Table S1). The DNA fragments of *MAM3* and *MGR1/CST2* were cloned into the pRS415-ADH vector (Mumberg *et al.*, 1995) using the In-Fusion cloning system (Clontech). The resulting vectors (and empty vectors) were introduced into the yeast WT and/or *mam3* mutant and used for measurement of Mg concentration.

Yeast cells were grown for 14 h in SD medium containing 3 mM $Mg^{2+}$ and then harvested by centrifugation. After washing four times with Milli Q water, cell pellets were dried at 70°C for at least 3 d. The concentration of Mg in the dried cells was measured as described in the previous sub-section.

## Expression analysis of *MGR1/CST2* by quantitative real-time polymerase chain reaction (qRT-PCR)

To examine the expression pattern of *MGR1/CST2*, 6-wk-old WT seedlings precultured in 1/10 strength Hoagland solution were transferred to a nutrient solution containing 0, 0.25, and 5 mM $Mg^{2+}$. After 3 d, roots and leaves were sampled for RNA

extraction with four biological replicates. Total RNA was extracted using an RNeasy Plant Mini Kit (Qiagen), and then converted to cDNA using ReverTra Ace qPCR RT Master Mix with gDNA Remover (Toyobo, Osaka, Japan). The expression of *MGR1/CST2* was determined by qRT-PCR with KOD SYBR qPCR Mix (Toyobo) on a real-time PCR machine (model no. CFX96; Bio-Rad) using the primers MGR1/CST2_qRT_F and MGR1/CST2_qRT_R (Table S1). Actin was used as an internal standard using the primers Actin_qRT_F and Actin_qRT_R (Table S1). The relative expression was normalized to that of actin using the ΔΔCt method.

To confirm the expression of *MGR1/CST2* mRNA in *cst2-2*, total RNA was isolated from rosette leaves of 3-wk-old WT and *cst2-2* plants using NucleoSpin RNA Plant (Takara, Shiba, Japan). First-strand cDNA was synthesized from the RNAs using the PrimeScript II 1st Strand cDNA Synthesis Kit (Takara). The *MGR1/CST2* and *TUB2* fragments were amplified from cDNA by PCR using the specific primers MGR1/CST2_RT-PCR_F and MGR1/CST2_RT-PCR_R for *MGR1/CST2*, and TUB2_RT-PCR_F and TUB2_RT-PCR_R for *TUB2* (Table S1). The *TUB2* fragment was used as an internal standard.

## Subcellular localization of CST2

MGR1/CST2-GFP, TTS-mCherry, and mCherry-AHA1 were transiently expressed in leaves of *N. benthamiana* grown in soil under the control of the 35S promoter. The full-length cDNA of each gene was amplified by PCR using the following primers: MGR1/CST2_SL_F and MGR1/CST2_SL_R for *MGR1/CST2*, TTS_SL_F and TTS_SL_R for *TTS*, and AHA1_SL_F and AHA1_SL_R for *AHA1* (Table S1). The amplified fragments were cloned into the *Nco*I and *Bsr*GI sites of the CaMV35S-sGFP(S65T)-NOS3′ and CaMV35S-mCherry-NOS3′ vectors. The cDNA of *MGR1/CST2-GFP*, *TTS-mCherry*, and *mCherry-AHA1* was amplified by PCR from the resulting vectors using the primers MGR1/CST2_SL_F and MGR1/CST2_SL_R for *MGR1/CST2-GFP*, TTS-mCherry_F and TTS-mCherry_R for *TTS-mCherry*, and mCherry-AHA1_F and mCherry-AHA1_R for *mCherry-AHA1* (Table S1). They were cloned into the pRI101-AN DNA vector downstream of 35S promoter using the In-Fusion cloning system (Takara). The resulting construct was introduced into *N. benthamiana* leaves using an *Agrobacterium*-mediated transformation method (Hayashi *et al.*, 2017; Inoue *et al.*, 2020). The *Agrobacterium* GV3101 strain was transformed with the vector and cultured at 28°C for *c.* 20 h. The agrobacteria were collected and resuspended in infection buffer including 10 mM Mes-KOH (pH 5.6) and 10 mM $MgCl_2$. Green fluorescent protein (GFP) and mCherry fluorescent signals from pavement cells were observed 4 d after the infiltration using a confocal laser microscope (FV10i; Olympus, Tokyo, Japan).

## Generation of transgenic plants

For functional complementation experiments, genomic fragments of the *MGR1/CST2* gene (*c.* 7 kbps), including the 5′ and 3′ noncoding regions, which include the promoter and

terminator, were amplified by PCR from WT genomic DNA using the primers gMGR1/CST2_F and gMGR1/CST2_R (Table S1). The DNA fragment was cloned into the *Sal*I site of the pCAMBIA1300 vector (Cambia).

For the promoter-GUS assay, the *GUS* gene was amplified from the pCAMBIA1303 vector (Cambia) using the primers GUS_F and GUS_R (Table S1). The DNA fragment was inserted into the site just before the stop codon of the *MGR1/CST2* gene in the construct for the complementation experiment using the In-Fusion cloning system.

For the generation of MGR1/CST2 overexpression plants, full length cDNA of the *MGR1/CST2* gene was amplified from cDNA by PCR using the primers MGR1/CST2_OE_F and MGR1/CST2_OE_R (Table S1). The cDNA fragment amplified was cloned into the *Sal*I site downstream of the 35S promoter of the pRI101-AN vector.

To examine the role of MGR1/CST2 in guard cells, we expressed *MGR1/CST2* in the *cst2* mutant under the control of the *MYB60* promoter, which is specifically expressed in the guard cells (Rusconi *et al.*, 2013). We first amplified the genomic fragments of the *MYB60* promoter using the primers pMYB60_F and pMYB60_R (Table S1), which were subsequently cloned into the *Hind*III/*Bam*HI site of pPZP211-35S-nosT, and the pPZP211-MYB60pro vector was generated. The cDNA of *GFP* and *MGR1/CST2-GFP* fusion were separately amplified using the primers GFP_MYB60_F and GFP_MYB60_R for *GFP*, and MGR1/CST2_MYB60_F and GFP_MYB60_R for *MGR1/CST2-GFP* (Table S1). The amplified DNA was inserted into the *Bam*HI site of the pPZP211-MYB60pro vector using the In-fusion cloning system.

The plasmids constructed as described here were transformed into the *Agrobacterium tumefaciens* GV3101 strain. The *Agrobacterium* was transformed into the *cst2-1* mutant using the floral dip method (Clough & Bent, 1998). Transgenic plants were selected by resistance against hygromycin or kanamycin and used for analysis. Transgenic lines were used for phenotypic analysis and observations as described in the following sub-sections.

### Promoter-GUS analysis

Whole individual plants, leaves, and roots were sampled from 1- to 3-wk-old seedlings for a promoter-GUS assay, as described previously (Hayashi *et al.*, 2020). The samples were fixed with 90% acetone for 20 min on ice, and then incubated in the GUS staining solution (0.5 mg ml$^{-1}$ 5-bromo-5-chloro-3-indolyl-β-D-glucuronide (X-Gluc), 0.5 mM $K_5[Fe(CN)_6]$, 0.5 mM $K_3[Fe(CN)_6]$, 50 mM sodium phosphate buffer (pH 7.0)) at 37°C for 14 h. After being washed with 70% ethanol and fixed in a 15% acetic acid and 85% ethanol solution, the GUS signal was observed using an upright microscope (Eclipse 50i; Nikon, Tokyo, Japan) and a charge-coupled device (CCD) camera (DS-5Mc-L2; Nikon). Tissue sections of the GUS-stained plants were obtained as described previously (Uchida *et al.*, 2012). To make plastic sections, samples were fixed in formalin/acetic acid/alcohol and embedded in Technovit 7100 resin (Heraeus Kulzer,

Wehrheim, Germany). Then, 4-μm sections were prepared and stained with 0.04% neutral red.

### Immunoblotting of plant proteins

Immunoblotting was performed using guard cell protoplasts (GCPs), mesophyll cell protoplasts (MCPs), leaves, and roots (Figs 2d,e, 3j, S1b, S4a, S5a). The GCPs and MCPs were prepared enzymatically from rosette leaves of 4- to 5-wk-old Arabidopsis plants, as described previously (Ueno *et al.*, 2005). Proteins were extracted from the cells and tissues according to methods described previously (Inoue *et al.*, 2008; Hayashi *et al.*, 2017). The protein samples were subjected to sodium dodecyl sulfate–polyacrylamide gel electrophoresis (SDS-PAGE). Immunoblotting was performed using the antibodies against MGR1/CST2, V-PPase and actin. Anti-MGR1/CST2 was raised against the recombinant MGR1/CST2 fragment as an antigen in a rabbit (Medical & Biological Laboratories, Nagoya, Japan). The cDNA of the *MGR1/CST2* C-terminal fragment (*MGR1/CST2 C-ter*) was amplified by PCR using the primers MGR1/CST2_C-ter_F and MGR1/CST2_C-ter_R (Table S1) and cloned into the *Bam*HI site of the pET30a vector (Novagen, Madison, WI, USA). The resulting construct was transformed into the *Escherichia coli* BL21 (DE3) strain. The recombinant MGR1/CST2 protein was expressed as a fusion protein to the His-tag (His-MGR1/CST2). The fusion protein was purified using the Profinity IMAC Ni-charged resin (Bio-Rad). The His-MGR1/CST2 protein was obtained by elution with imidazole and was used as an antigen to immunize the rabbit. Anti-actin (Sigma-Aldrich) and anti-V-PPase (Cosmo Bio, Tokyo, Japan) antibodies were purchased. Experiments repeated three times on separate occasions gave similar results.

### Chl fluorescence-based photosynthesis analysis

For measurement of the quantum yield of electron transfer to PSII (ΦPSII), Chl fluorescence yield was measured with a FluorCAM (Photon System Instruments) in plants grown in soil under light at 200 μmol m$^{-2}$ s$^{-1}$ for 5 wk. Steady-state fluorescence ($F_s$) was measured in actinic light at 200 μmol m$^{-2}$ s$^{-1}$. Maximum fluorescence ($F_m'$) was determined by a saturating light pulse (*c.* 2000 μmol m$^{-2}$ s$^{-1}$) under actinic light at 200 μmol m$^{-2}$ s$^{-1}$. ΦPSII was calculated as ($F_m'-F_s)/F_m$.

### Statistical analysis

All experiments were independently repeated at least twice. Statistical analyses were performed using Tukey's test.

## Results

### Isolation and physiological characterization of a mutant defective in stomatal opening

We previously performed a large-scale genetic screening of Arabidopsis mutants using infrared thermography to improve our understanding of the mechanisms involved in stomatal opening

(Inoue *et al.*, 2017). We obtained several mutants (designated *closed stomata* (*cst*)) which exhibited higher leaf temperatures than WT plants due to their impaired stomatal opening. We have functionally characterized the first mutant, *cst1*, in a previous study, and found that brassinosteroids are involved in light-dependent stomatal opening (Inoue *et al.*, 2017). In the present study, we report on the second mutant, *cst2-1*, which also showed higher leaf temperatures and retarded growth (Fig. 1a). We isolated leaf epidermal fragments from dark-adapted plants and measured light-dependent stomatal opening. Stomata in the epidermis of WT plants barely opened in the dark, but opened wide in response to light (Fig. 1b). By contrast, stomata in the epidermis of *cst2-1* plants exhibited a lesser degree of opening than those of the WT under both light and dark conditions (Fig. 1b), but the difference in stomatal opening between *cst2-1* and WT was larger under light conditions.

The *cst2-1* mutant showed reduced photosynthetic electron transfer to PSII compared to the WT under soil growth conditions (Fig. 1c). The growth of *cst2-1* was greatly decreased compared with the WT (Fig. 1d).

### Gene mapping and complementation test

In order to map the gene responsible for the *cst2-1* phenotype, we performed map-based cloning and sequence analysis using a next-generation sequencer. As a result, we identified a single nucleotide substitution from guanine (G) to adenine (A) at the sixth intron splicing acceptor site of the *AT4G14240* gene, (Fig. S1). This gene was also recently identified as *Magnesium Release 1* (*MGR1*) (Tang *et al.*, 2022). No MGR1/CST2 protein was detected in the mutants in a Western blot analysis (Fig. S1b). To confirm this mapping result, we performed a complementation test by
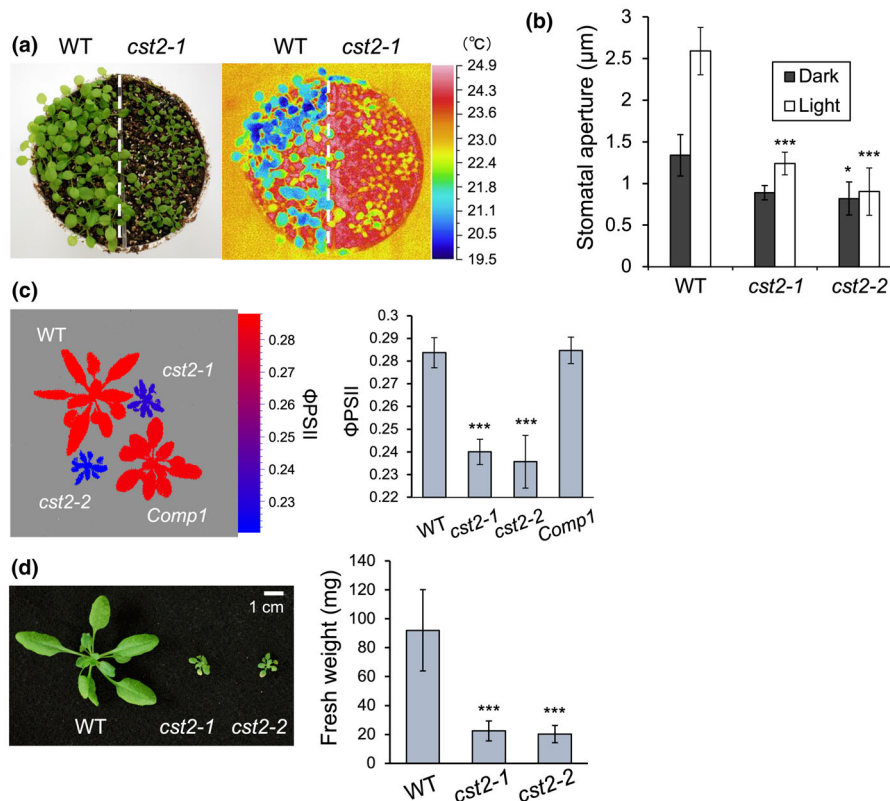


**Fig. 1** Isolation and physiological characterization of *cst2* mutants of Arabidopsis. (a) Infrared thermal images of Arabidopsis wild-type (WT) and *cst2-1* plants during growth under light. Plants were grown for 3 wk. Thermal images were taken at 3–4 h after the start of the light period. (b) Light-dependent stomatal opening in WT and *cst2* mutant plants. Epidermal fragments were isolated from dark-adapted plants and suspended in a potassium chloride (KCl) based buffer. The epidermal fragments were irradiated with mixed light (red light (50 μmol m$^{-2}$ s$^{-1}$) and blue light (10 μmol m$^{-2}$ s$^{-1}$)) for 3 h. Stomatal apertures were measured using microscopy. Data represent the mean ± SD of triplicate experiments. Each experiment used 30 stomata. Asterisks indicate statistically significant differences from the corresponding WT control, calculated using two-way analysis of variance (ANOVA) with Tukey's multiple comparisons test (*, $P < 0.05$; ***, $P < 0.001$). (c) Photosynthetic activity of WT and *cst2* mutant plants. The quantum yield of electron transfer to photosystem II (ΦPSII) was measured in WT, *cst2-1*, *cst2-2* and complementation line no. 1 (comp1) grown under 200 μmol m$^{-2}$ s$^{-1}$ light conditions for 5 wk. Measurements were made after exposure of leaves to actinic light of 200 μmol m$^{-2}$ s$^{-1}$ for 5 min. Left panel, image of ΦPSII; right panel, photosynthetic activity. Data are means ± SD ($n = 3$). Asterisks indicate statistically significant differences from the corresponding WT control, calculated using one-way ANOVA with Dunnett's multiple comparisons test (***, $P < 0.001$). (d) Growth (left) and fresh weight (right) of WT and *cst2* mutants. Plants were grown on soil for 4 wk. The aerial parts were harvested and the fresh weight was recorded. Data are means ± SD ($n = 20$). Asterisks indicate statistically significant differences from the corresponding WT control, calculated using one-way ANOVA with Dunnett's multiple comparisons test (***, $P < 0.001$). Bar, 1 cm.

introducing the WT *MGR1/CST2* gene into the *cst2-1* mutant. Analysis with three independent lines (Comp1 to Comp3) showed that *MGR1/CST2* completely restored the growth defect and stomatal opening of the *cst2-1* mutant (Fig. S1). Furthermore, we obtained a T-DNA insertion line (GABI_322H07), which we designated *cst2-2* (Fig. S1). There was no expression of the *MGR1/CST2* gene and protein in this line (Fig. S1). Furthermore, *cst2-2* showed similar phenotypes to *cst2-1* in terms of growth, stomatal opening and photosynthesis (Fig. 1b–d), indicating that *cst2-2* is also a knockout mutant of *MGR1/CST2*. These observations indicate that all phenotypes of *cst2* are caused by mutations in the *MGR1/CST2* gene.

To examine whether the stomatal closure in *cst2* is associated with a signal from the guard cells, we compared the effects of the fungal toxin fusicoccin (FC) on stomatal opening in WT and *cst2* mutant plants. Fusicoccin directly activates the plasma membrane $H^+$-ATPase and induces stomatal opening in the dark (Kinoshita *et al.*, 2001). When the epidermal fragments from WT, *cst2-1* and *cst2-2* leaves were exposed to FC in the dark, the application of FC induced large stomatal opening in the WT epidermis but not in the epidermis of either *cst2* mutant (Fig. S2). These results suggest that signaling for stomatal opening in the *cst2* guard cells may be impaired downstream of the $H^+$-ATPase.

## Phylogenetic analysis of MGR1/CST2

*MGR1/CST2* encodes an uncharacterized protein with a transmembrane Domain of Unknown Function 21 (DUF21) and a cytosolic cystathionine-β-synthase (CBS)-pair domain (Chen *et al.*, 2021) (Fig. S3a). In the Arabidopsis genome, there are six homologs of MGR1/CST2, with similarity ranging from 43.6 to 82.4% (Fig. S3b). A BLAST search revealed that domains of MGR1/CST2 are found in archaea, bacteria, fungi, algae, plants, and animals (Fig. S3c). Among them, bacterial homologs $Co^{2+}$ resistance (Cor)B and Magnesium Protection Factor (Mpf)A were reported to mediate $Mg^{2+}$ efflux (Gibson *et al.*, 1991; Armitano *et al.*, 2016; Trachsel *et al.*, 2019). A yeast homolog of MGR1/CST2, MAM3 (Fig. S3c) was reported to be associated with manganese (Mn) homeostasis and located to the tonoplast, but its exact role in $Mg^{2+}$ homeostasis is unknown (Yang *et al.*, 2005). Animal homolog ACDPs/CNNMs were also implicated in $Mg^{2+}$ transport, although it was unclear whether CNNM proteins are $Mg^{2+}$ transporters or regulators of other $Mg^{2+}$ transporters (Arjona & de Baaij, 2018; Funato *et al.*, 2018). Recently, archaeal CorB was found to exhibit $Mg^{2+}$ transport activity *in vitro* (Chen *et al.*, 2021).

## MGR1/CST2-derived $Mg^{2+}$ accumulation and subcellular localization of MGR1/CST2

To test whether MGR1/CST2 and yeast MAM3 are able to transport $Mg^{2+}$ like the homologs in other organisms described in the previous subsection (Fig. S3c), we performed a yeast assay using the yeast mutant *mam3*. When yeast was grown on SD medium containing 3 mM $Mg^{2+}$, the *mam3* knockout mutant showed reduced Mg accumulation compared to the WT (Fig. 2a: empty/

WT vs empty/*mam3*). This mutant phenotype was completely recovered by introduction of the WT *MAM3* gene and of the Arabidopsis *MGR1/CST2* gene (Fig. 2a: Empty/*mam3* vs *MAM3/mam3* and *MGR1/CST2/ mam3*). These results indicate that MGR1/CST2 functions as an ortholog of MAM3, and that both MAM3 and MGR1/CST2 are able to transport $Mg^{2+}$.

We then investigated the subcellular localization of MGR1/CST2 by transiently expressing MGR1/CST2-GFP fusion gene with a tonoplast marker (tonoplast target signal (*TTS*)-*mCherry*) and plasma membrane marker (*mCherry-AHA1*) in *N. benthamiana* leaves (Fig. 2b). The result showed that the fluorescence signal from MGR1/CST2-GFP was well merged with the tonoplast marker. These results indicate that, similar to MAM3, MGR1/CST2 protein is also localized to the tonoplast.
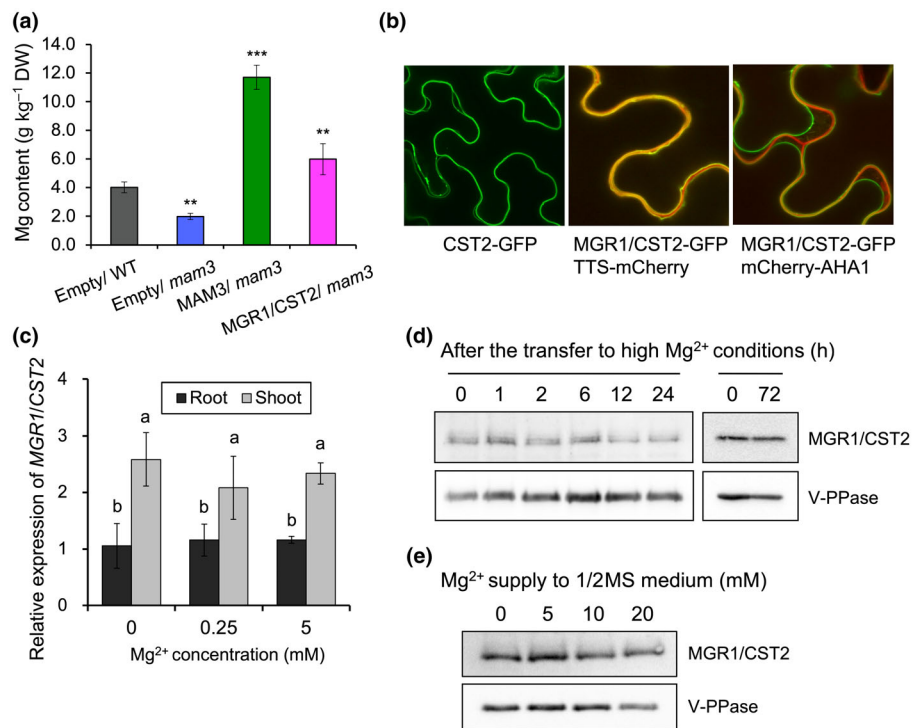
## Expression pattern of *MGR1/CST2*

We examined the expression pattern of *MGR1/CST2* using qRT-PCR. The expression of *MGR1/CST2* was higher in the leaves than in the roots (Fig. 2c). The expression in both the roots and shoots did not respond to $Mg^{2+}$ deficiency (0 mM) or excess (5 mM) (Fig. 2c). Western blot analysis showed that MGR1/CST2 protein accumulation was not altered by high $Mg^{2+}$ (20 mM) for up to 72 h (Fig. 2d). Furthermore, accumulation of the MGR1/CST2 protein did not change in response to a 5, 10 or 20 mM $Mg^{2+}$ supply compared with a 0 mM $Mg^{2+}$ supply (Fig. 2e). These results indicate that MGR1/CST2 is constitutively expressed at both transcriptional and protein levels.

We further investigated the expression patterns of *MGR1/CST2* using transgenic plants expressing the *GUS* reporter gene under the control of the native *MGR1/CST2* promoter. Consistent with the qRT-PCR results (Fig. 2c), the GUS signal was observed to be ubiquitous in both the roots and leaves, with a stronger signal in the leaves (Fig. 3a–c,f,g). In the leaf, a strong signal was observed in the guard cells (Fig. 3d,e,h) and vascular bundle tissues (Fig. 3c,d,f,h,i). Expression of the MGR1/CST2 protein was also confirmed by Western blot analysis in guard cells, mesophyll cells, leaves, and roots (Fig. 3j).

## Effect of different $Mg^{2+}$ concentrations on growth of *cst2* mutants and overexpression lines

To investigate the role of MGR1/CST2 in $Mg^{2+}$ homeostasis, we compared the hydroponic growth between the WT and two independent *cst2* mutants at different $Mg^{2+}$ concentrations, including 0.25, 1, and 5 mM. When the WT and *cst2* mutants were grown for 4 wk at 0.25 mM $Mg^{2+}$, the growth of both the roots and shoots were very similar (Fig. 4a). However, at 1 mM $Mg^{2+}$ (a normal concentration for hydroponic solution) and 5 mM $Mg^{2+}$, the growth of both the roots and shoots of *cst2* mutants was significantly decreased compared with the WT (Fig. 4a–c). We further tested whether this response was specific to high $Mg^{2+}$ concentrations by exposing the plants to excess concentrations of other ions on ½MS agar medium. The results showed that the growth difference between the WT and *cst2* mutants was not observed in other excess ion conditions – only at high $Mg^{2+}$

**Fig. 2** Magnesium (Mg$^{2+}$) transport activity of MGR1/CST2, subcellular localization and expression pattern of *MGR1/CST2*. (a) Magnesium concentration in transgenic yeast cells. Yeast mutant plants (*mam3*) expressing *MAM3*, *MGR1/CST2* cDNA or empty vector were grown on SD medium containing 3 mM Mg$^{2+}$ for 14 h. The Mg concentration in yeast was determined by inductively coupled plasma mass spectrometry (ICP-MS). Data represent the mean ± SD (*n* = 5). Asterisks indicate statistically significant differences from the empty vector/wild-type (WT), calculated using one-way analysis of variance (ANOVA) with Dunnett's multiple comparisons test (**, *P* < 0.01; ***, *P* < 0.001). DW, dry weight. (b) Subcellular localization of MGR1/CST2-GFP. *MGR1/CST2-GFP* was expressed alone (left) or co-expressed with tonoplast target signal (*TTS*)-*mCherry* (center) or *mCherry-AHA1* (right) in leaf epidermal cells of *Nicotiana benthamiana*. Fluorescent images were obtained using a confocal laser microscope. (c) Expression pattern of *MGR1/CST2* in different organs of Arabidopsis (Col-0). Seedlings (6 wk old) precultured in 1/10 strength Hoagland solution were exposed to a nutrient solution containing 0, 0.25, and 5 mM Mg$^{2+}$ for 3 d, and the roots and leaves were sampled for RNA expression. The expression of *MGR1/CST2* was determined by quantitative real-time PCR (qRT-PCR). Expression relative to roots not exposed to Mg$^{2+}$ is shown. Data are means ± SD (*n* = 4). Different letters indicate significant differences at *P* < 0.01 according to the Tukey–Kramer test. (d) Time-dependent change of MGR1/CST2 protein in response to high Mg$^{2+}$ concentrations. Wild-type plants were grown on ½ Murashige & Skoog (½MS) agar medium (containing 0.75 mM Mg$^{2+}$) for 2 wk, and then transferred onto ½MS agar medium supplemented with 20 mM Mg$^{2+}$. Proteins were extracted from rosette leaves at the indicated time points and subjected to immunoblotting using MGR1/CST2 and V-PPase antibodies. (e) Magnesium (Mg$^{2+}$) concentration-dependent MGR1/CST2 protein expression. Plants were grown on ½MS agar medium containing the indicated Mg$^{2+}$ concentrations for 2 wk. Protein samples were prepared from rosette leaves and subjected to immunoblotting using MGR1/CST2 and V-PPase antibodies.

concentrations (Fig. S4). The large growth difference between the WT and *cst2* mutants was also observed following supplementation with excess MgCl$_2$, indicating that mutant phenotype is caused by high Mg$^{2+}$ rather than anions.

We also generated *MGR1/CST2* overexpression lines. The overexpression lines showed a higher accumulation of MGR1/CST2 protein (Fig. S5a). Overexpression of *MGR1/CST2* significantly enhanced tolerance to high Mg$^{2+}$ concentrations compared with the WT (Fig. S5b). At Mg$^{2+}$ concentrations > 35 mM, the overexpression lines were able to survive, whereas the WT died. In addition, both overexpression lines showed enhanced light-dependent stomatal opening compared to the WT (Fig. S5c).

We compared the Mg concentration in the leaves between the WT and *cst2* mutant plants. The results showed that at normal Mg$^{2+}$ concentrations on ½MS agar medium (0.75 mM), the shoot Mg concentration was similar between the WT and the

*cst2* mutant (Fig. 4d). However, at high Mg$^{2+}$ concentrations (0.75 + 5 mM), the mutants exhibited lower Mg concentrations than the WT. This decrease in Mg accumulation could be attributed to disrupted Mg homeostasis in the cells. Higher Mg concentrations in the cytosol in the mutant may downregulate transporter genes involved in Mg$^{2+}$ uptake, though further investigation is required.

## Mg$^{2+}$ homeostasis is associated with stomatal opening

To link Mg$^{2+}$ homeostasis with stomatal opening, we investigated the light-dependent stomatal opening of *cst2* mutants and WT plants grown in hydroponic solution with various Mg$^{2+}$ concentrations. Stomata in the WT leaves opened to a similar extent in response to Mg$^{2+}$ concentrations from 0.05 to 5 mM under light conditions. However, stomata in the *cst2-1* leaves opened only at Mg$^{2+}$ concentrations from 0.05 to 0.2 mM under light
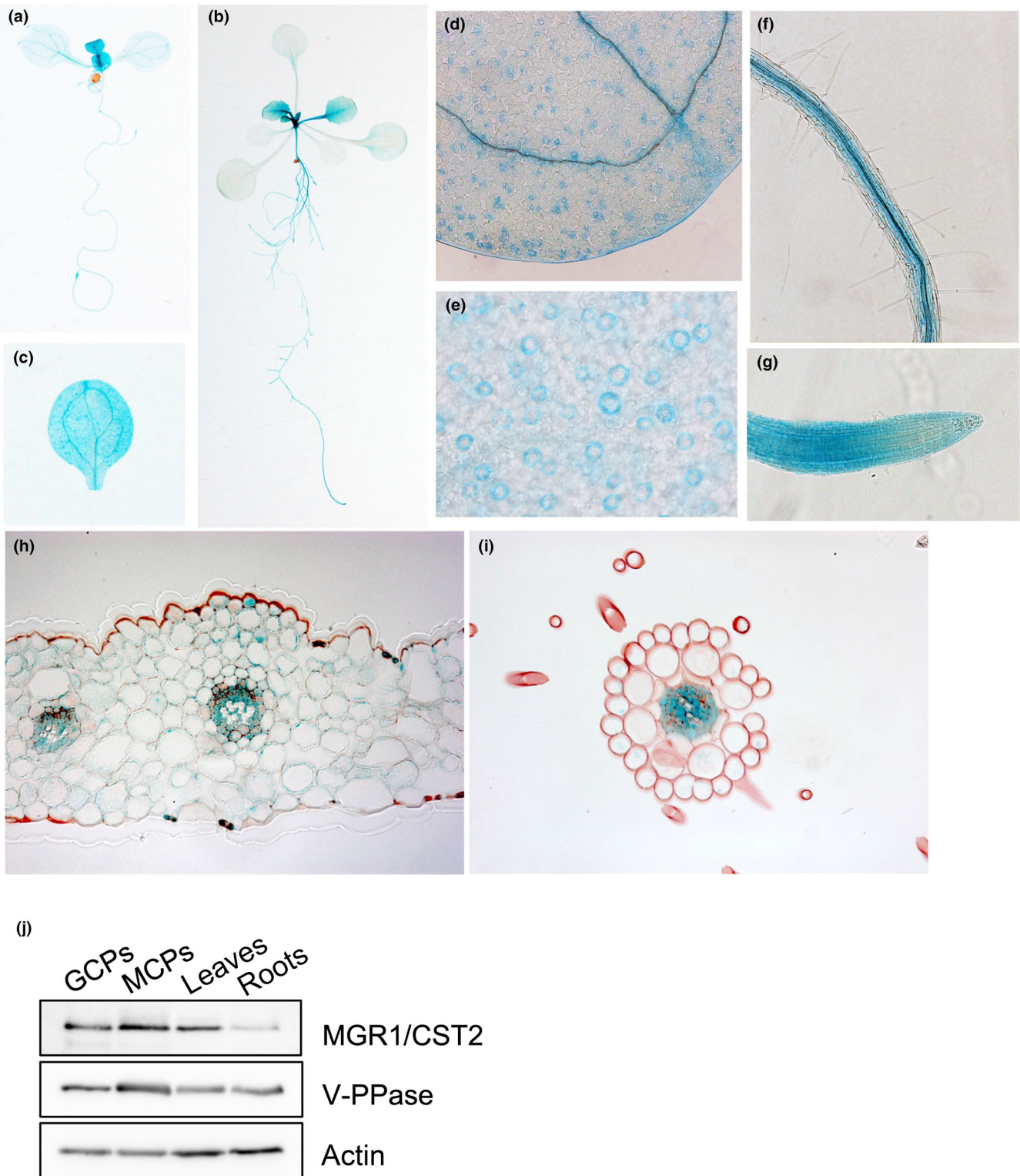
**Fig. 3** Tissue specificity of MGR1/CST2 expression in Arabidopsis. (a–i) Expression patterns of *MGR1/CST2* in different organs and tissues. Transgenic Arabidopsis plants carrying *MGR1/CST2 promoter-GUS* were grown on ½ Murashige & Skoog (½MS) agar medium and used for the GUS assay. (a) A young (1-wk-old) plant. (b) A 3-wk-old plant. (c) Cotyledon. (d) Magnified image of the cotyledon. (e) Magnified image of the leaf surface of a true leaf. (f) Root. (g) Primary root tip. (h, i) Cross section of a true leaf (h) and the primary root (i). Red coloring is cell-wall staining by Nile red. (j) Expression of MGR1/CST2 protein in different cells and tissues. Wild-type (WT) plants were grown on soil for 4 wk, and different cell types were isolated. Immunoblotting was performed using antibodies against MGR1/CST2, V-PPase, and actin antibodies. GCPs, guard cell protoplasts; MCPs, mesophyll cell protoplasts.
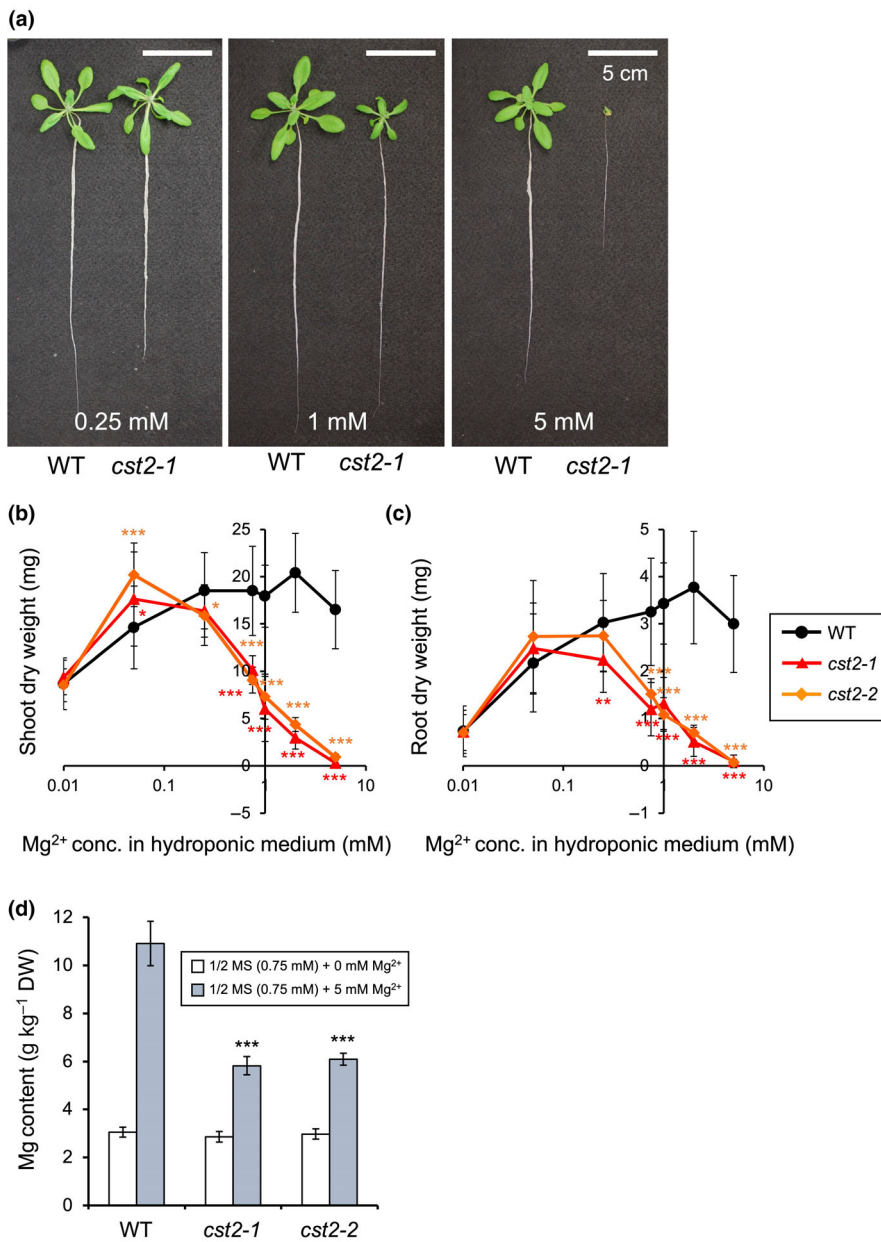
**Fig. 4** Phenotypic characterization of *cst2* mutants at different magnesium ($Mg^{2+}$) concentrations. (a–c) Growth of wild-type (WT) and *cst2-1* mutant plants at various $Mg^{2+}$ concentrations in hydroponic medium. Plants of Arabidopsis were grown on ½ Murashige & Skoog (½MS) agar medium for 7 d, after which they were transferred to a nutrient solution containing 0.25, 1 or 5 mM $Mg^{2+}$ (a). After 5 wk, the seedlings were photographed. The plots show the dry weight of shoots (b) and roots (c) of WT and *cst2* plants grown in hydroponic solution with different $Mg^{2+}$ concentrations. Four weeks after the transfer, the shoots and roots were harvested. Data represent the mean ± SD ($n = 16$). Asterisks indicate statistically significant differences from the corresponding WT control, calculated using two-way analysis of variance (ANOVA) with Tukey's multiple comparisons test ($*$, $P < 0.05$, $**$, $P < 0.01$; $***$, $P < 0.001$). (d) Shoot Mg concentration in WT, *cst2-1*, and *cst2-2* plants. The plants were grown on ½MS agar medium (containing 0.75 mM $Mg^{2+}$), with or without the addition of 5 mM $Mg^{2+}$, for 3 wk. Data represent the mean ± SD ($n = 6$). Asterisks indicate statistically significant differences from the corresponding WT control, calculated using two-way ANOVA with Tukey's multiple comparisons test ($***$, $P < 0.001$).

conditions (Fig. 5a). Stomatal opening in *cst2* mutants was completely suppressed at $Mg^{2+}$ concentrations of 0.75 mM or higher in the hydroponic solutions.

We further investigated $Mg^{2+}$-dependent stomatal opening in a time-dependent manner. The stomatal opening abilities of the mutants started to decrease at 24 h after the plants were transferred from 0.2 to 5 mM $Mg^{2+}$ (Fig. 5b). By contrast, the stomatal opening ability of the WT hardly changed over time under the same conditions. We also compared the stomatal conductance and photosynthetic rate between the WT and *cst2* mutants. The magnitude and rate of stomatal conductance were reduced in *cst2* mutants compared to those in the WT (Fig. 5c). The photosynthetic rate in *cst2* mutant leaves was also reduced (Fig. 5d). These results suggest that $Mg^{2+}$ homeostasis is important for stomatal opening and photosynthesis.

### Role of $Mg^{2+}$ and MGR1/CST2 expression in guard cells in stomatal opening

In the stomatal opening bioassay shown in Fig. 1(b), KCl-based buffer was used since $K^+$ is known to be required for stomatal opening under light conditions (Schroeder *et al.*, 2001; Shimazaki *et al.*, 2007; Marten *et al.*, 2010; Inoue *et al.*, 2017). To test whether $Mg^{2+}$ has a similar role to $K^+$ in stomatal opening, we performed a stomatal opening bioassay with $Mg^{2+}$, and without $K^+$, in the buffer, using WT epidermal cells. The result showed that, similar to $K^+$, $Mg^{2+}$ was able to stimulate stomatal opening in response to light (Fig. 6a). Interestingly, the light-induced stomatal opening was further promoted in the presence of both $Mg^{2+}$ and $K^+$ (Fig. 6a). However, stomata in the *cst2* mutant epidermis did not open in the manner observed in the
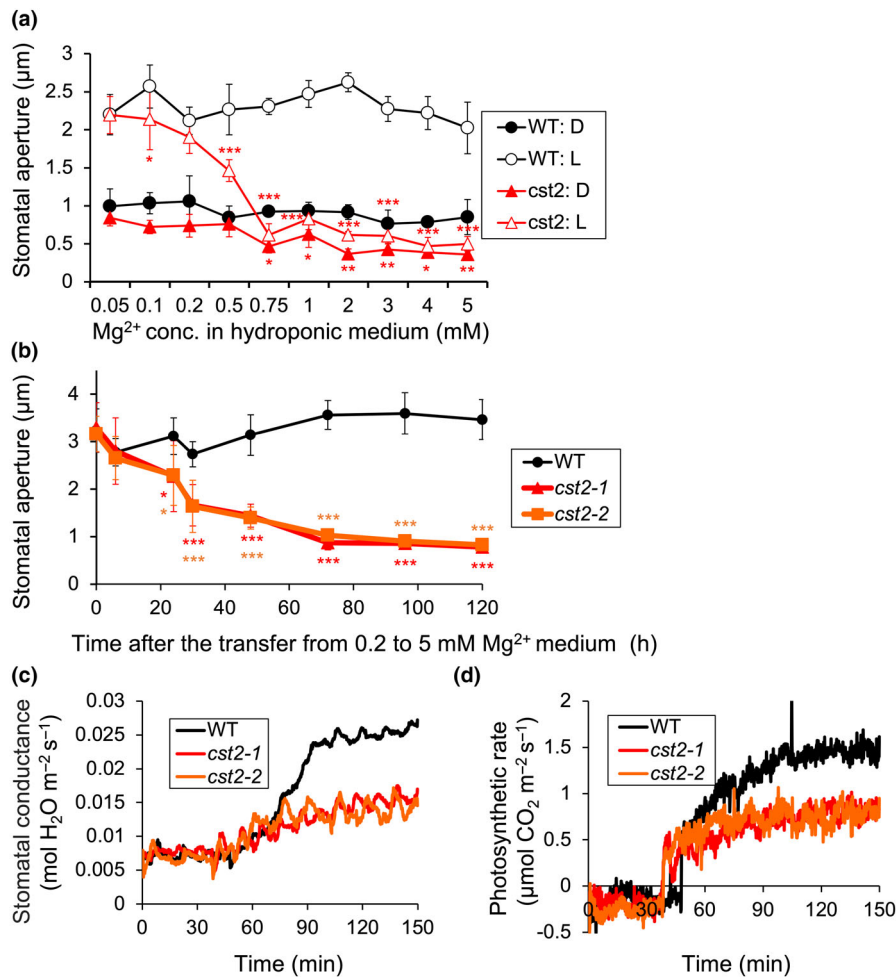
**Fig. 5** Time-dependent change in stomatal opening in response to high magnesium ($Mg^{2+}$) concentrations in Arabidopsis. (a) Light- and $Mg^{2+}$-dependent stomatal opening in wild-type (WT) and *cst2-1* mutant plants. Arabidopsis plants were grown in a hydroponic solution with various $Mg^{2+}$ concentrations for 28–32 d before being subjected to stomatal aperture measurement. Epidermal fragments were isolated from dark-adapted plants, suspended in a potassium chloride (KCl)-based buffer, and used for measurement. The epidermal fragments were irradiated with mixed light (red light (50 μmol m$^{-2}$ s$^{-1}$) and blue light (10 μmol m$^{-2}$ s$^{-1}$) for 3 h. Stomatal apertures were measured using microscopy. D, dark conditions; L, light conditions. Data represent the mean ± SD of three to five experiments. Each experiment used 30 stomata. Asterisks indicate statistically significant differences from the corresponding WT control, calculated using two-way analysis of variance (ANOVA) with Tukey's multiple comparisons test (*, $P < 0.05$; **, $P < 0.01$; ***, $P < 0.001$). (b) Time-course of stomatal opening abilities of the WT and *cst2* mutants in response to high $Mg^{2+}$ treatment. Plants were grown in a hydroponic solution containing 0.2 mM $Mg^{2+}$ for 4 wk, and then transferred to a solution containing 5 mM $Mg^{2+}$ and grown for a further 5 d. Epidermal fragments were immediately isolated from the rosette leaves sampled at the indicated times, and stomatal apertures were determined by microscopy. Data represent the mean ± SD of four experiments. Each experiment used 30 stomata. Asterisks indicate statistically significant differences from the corresponding WT control, calculated using two-way ANOVA with Tukey's multiple comparisons test (*, $P < 0.05$; ***, $P < 0.001$). (c, d) Changes in stomatal conductance (c) and photosynthetic rate (d) in response to light in leaves of WT and *cst2* mutant plants. The plants were grown for 4 wk in a hydroponic solution containing 0.2 mM $Mg^{2+}$, and then transferred to a hydroponic solution containing 5 mM $Mg^{2+}$ for a further 5 d. The plants were kept in the dark overnight before measurement on the morning of the fifth day. White light at 1000 μmol m$^{-2}$ s$^{-1}$ was applied to the upper surface of the leaf. Experiments repeated on two occasions gave similar results.

WT in the presence of $Mg^{2+}$ alone or both $Mg^{2+}$ and $K^+$ (Fig. 6b). These results suggest that, similar to $K^+$, $Mg^{2+}$ is also able to increase the osmotic pressure for stomatal opening and that this $Mg^{2+}$ function is associated with MGR1/CST2 in the guard cells.

To further investigate the direct role of MGR1/CST2 expression in guard cells in stomatal opening, we generated transgenic plants expressing *GFP* or *MGR1/CST2-GFP* fusion gene under the control of a guard cell-specific *MYB60* promoter in the *cst2-1* background (Rusconi *et al.*, 2013). The bioassay showed that the light-induced stomatal opening was partially restored in the

guard cells harboring *MGR1/CST2-GFP* fusion gene, but not in those harboring *GFP* alone (Fig. 6c). These results directly indicate that MGR1/CST2 expression in the guard cells plays an important role in stomatal opening.

## Discussion

Stomatal opening in plant leaves is caused by the swelling of a pair of guard cells, which is achieved by increasing cell volume through ion accumulation followed by water influx (Shimazaki *et al.*, 2007; Inoue & Kinoshita, 2017). Until now, it has been reported that in
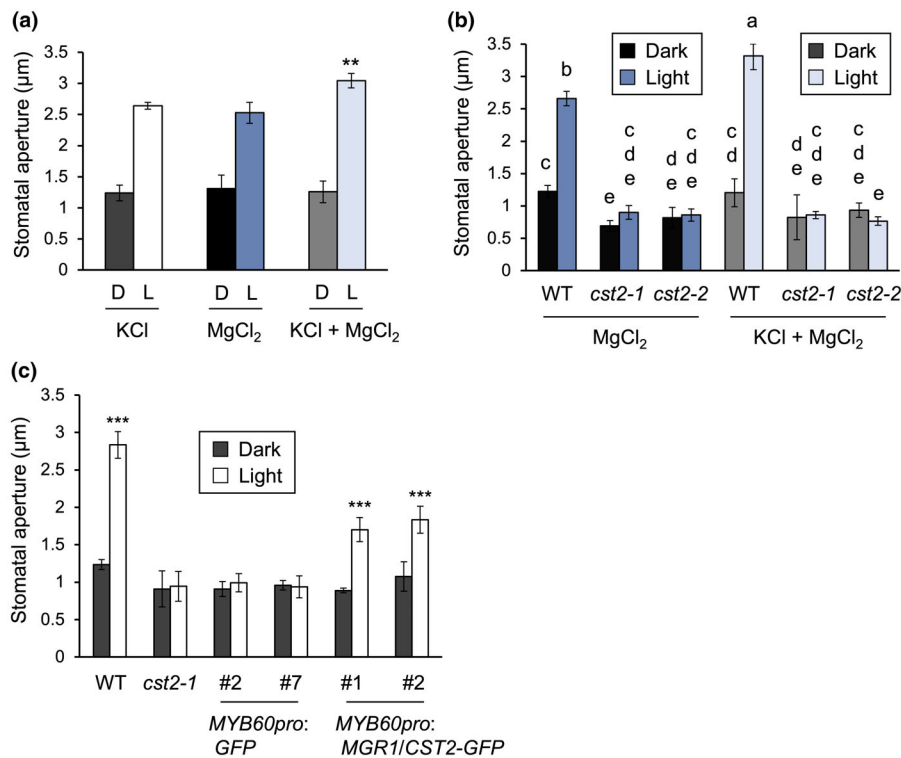
**Fig. 6** Role of magnesium ($Mg^{2+}$) and MGR1/CST2 expression in guard cells in the light-induced stomatal opening in Arabidopsis. (a) Effect of $Mg^{2+}$ concentrations on light-induced stomatal opening. Epidermal fragments were isolated from dark-adapted Arabidopsis plants grown in soil for 4 wk, followed by immersion in potassium chloride (KCl)-based buffer, magnesium chloride ($MgCl_2$)-based buffer, or $KCl/MgCl_2$-based buffer. D, dark conditions; L, light conditions. (b) Effect of $Mg^{2+}$ concentrations on light-induced stomatal opening in the wild-type (WT) and *cst2* mutants. Epidermal fragments of WT and *cst2* mutant leaves were isolated and suspended in $MgCl_2$-based buffer and $KCl/MgCl_2$-based buffer. (c) Light-dependent stomatal opening in WT, *cst2-1* mutant, and *cst2-1* plants harboring a transgene with the *MYB60pro:GFP* (no. 2 and no. 7) or the *MYB60pro:MGR1/CST2-GFP* (no. 1 and no. 2) constructs. Epidermal fragments were isolated from dark-adapted plants and suspended in a potassium chloride (KCl) based buffer. The epidermal fragments were irradiated with mixed light (red light (50 $\mu$mol m$^{-2}$ s$^{-1}$) and blue light (10 $\mu$mol m$^{-2}$ s$^{-1}$)) for 3 h. Stomatal apertures were measured using microscopy. Data represent the mean $\pm$ SD of five (a), four (b) and three (c) replicates. Each experiment used 30 stomata. Asterisks indicate statistically significant differences from the corresponding KCl treatment (a) and the corresponding *cst2-1* (c), calculated using two-way analysis of variance (ANOVA) with Tukey's multiple comparison test (**, $P < 0.01$; ***, $P < 0.001$). Different letters indicate significant differences at $P < 0.05$ according to the Tukey–Kramer test.

guard cells the accumulation of ions including $K^+$, $Cl^-$, nitrate ($NO^{3-}$), and malate$^{2-}$ in the vacuoles makes a large contribution to their increase in volume (Eisenach & De Angeli, 2017; Inoue & Kinoshita, 2017; Martinoia, 2018). In the present study, through mutant screening and gene mapping, we identified a gene, *MGR1/CST2*, encoding a tonoplast-localized $Mg^{2+}$ transporter. MGR1 was found to be involved in tolerance to high $Mg^{2+}$ concentrations (Tang *et al.*, 2022). However, we found that it is also involved in stomatal opening via regulation of $Mg^{2+}$. MGR1/CST2 is highly expressed in guard cells (Fig. 3d,e,h). Knockout of this gene resulted in stomatal closure, especially under high $Mg^{2+}$ concentrations (Fig. 5a–c), whereas its overexpression enhanced stomatal opening and tolerance to high $Mg^{2+}$ concentrations (Fig. S5). Furthermore, specific expression of *MGR1/CST2* in the guard cells was able to rescue the stomatal opining of the mutant (Fig. 6c). These results consistently support the involvement of MGR1/CST2 in stomatal opening (Fig. 7).

There are at least three possibilities for the involvement of MGR1/CST2 in stomatal opening. The first is that MGR1/CST2 mediates the transport of $Mg^{2+}$ into the vacuoles of guard cells (Fig. 7). It has been reported that $K^+$ contributes primarily to the

increase in turgor pressure in guard cells for stomatal opening (Schroeder *et al.*, 2001; Roelfsema & Hedrich, 2005; Shimazaki *et al.*, 2007; Marten *et al.*, 2010; Inoue & Kinoshita, 2017). Interestingly, we found in the present study that $Mg^{2+}$ has a similar role to $K^+$ in the stomatal opening (Fig. 6a). Therefore, knockout of *MGR1/CST2* failed to sequester $Mg^{2+}$ into the vacuoles, which is necessary for the increase in turgor pressure required for guard-cell swelling. This is supported by the finding that stomata in the isolated epidermis of *cst2* plants exhibited impaired light- and FC-dependent stomatal opening (Figs 1b, S2) as well as the finding that specific expression of *MGR1/CST2* in the guard cells partially rescued the stomatal opening of the mutant (Fig. 6c). Furthermore, MGR1/CST2-mediated stomatal opening was observed at a wide range of Mg concentrations, although it did not occur at low $Mg^{2+}$ concentrations (Fig. 5a).

The second possibility is that $Mg^{2+}$ homeostasis in the guard cells affects other components involved in stomatal opening (Fig. 7). Although $Mg^{2+}$ is an essential element for plant growth and development (Chen *et al.*, 2018), excess $Mg^{2+}$ in the cytosol due to a lack of vacuolar sequestration may cause toxicity, which affects other events involved in stomatal opening. In fact, it was
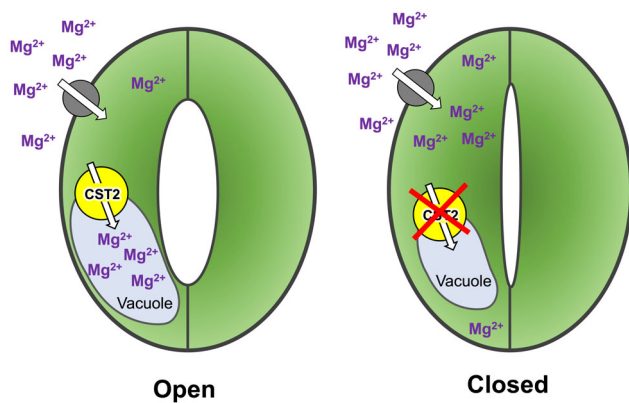
**Fig. 7** Schematic representation of the role of MGR1/CST2 in stomatal opening in Arabidopsis. The magnesium ($Mg^{2+}$) concentration in the cytosol of guard cells is maintained at a steady level in several different ways. One way is to sequester $Mg^{2+}$ into the vacuole via tonoplast-localized MGR1/CST2 to maintain $Mg^{2+}$ homeostasis, which is important for stomatal opening (left). Knockout of *MGR1/CST2* results in stomatal closure due to high $Mg^{2+}$ concentrations in the cytosol of the guard cells under high $Mg^{2+}$ conditions (right).

reported that excess $Mg^{2+}$ inhibits photosynthetic activity through affecting the stromal pH (Huber & Maury, 1980; Wu *et al.*, 1991). Because guard cell photosynthesis provides ATP and/or reducing equivalents, which are the fuel for stomatal opening (Tominaga *et al.*, 2001; Suetsugu *et al.*, 2014; Santelia & Lawson, 2016), inhibition of guard cell photosynthesis caused by high $Mg^{2+}$ conditions may result in stomatal closure. In addition, $Mg^{2+}$ can form chelates with malate and citrate, so free carboxylates are reduced in *cst2* mutant guard cells, which may affect energy metabolism important for stomatal opening (Martinoia, 2018).

The third possibility is that disruption of the $Mg^{2+}$ homeostasis in cells other than guard cells induces suppression of stomatal opening. This possibility is supported by our observation that that specific expression of *MGR1/CST2* in the guard cells of the epidermal tissue did not fully complement stomatal opening in the mutant (Fig. 6c). In fact, a defect in mesophyll cell photosynthesis could cause a $CO_2$ increase in leaves, which induces stomatal closure (Shimazaki *et al.*, 2007; Inoue & Kinoshita, 2017). Most previous studies of stomatal opening have focused only on the signaling within a guard cell, and the interaction between guard cells and other cells has hardly been investigated, except for a few studies on phytohormone abscisic acid (ABA) and $CO_2$ (Assmann, 1988; Shimazaki *et al.*, 2007; Kuromori *et al.*, 2018). Our study suggests that the maintenance of $Mg^{2+}$ homeostasis in other cells also plays an important role in stomatal opening, although the exact mechanisms remain to be examined in the future. Taken together, it seems that MGR1/CST2 plays an important role in stomatal opening via multiple functions. Nevertheless, further investigation is required to examine these possibilities.

MGR1/CST2 homologs such as MpfA, CorB, and CNNMs are present in archaea, bacteria, and animals and have been associated with the export of $Mg^{2+}$ from the cell (Gibson *et al.*, 1991; Yamazaki *et al.*, 2013; Armitano *et al.*, 2016; Trachsel

*et al.*, 2019; Chen *et al.*, 2021), indicating that $Mg^{2+}$ transport by MGR1/CST2-type transporters is evolutionarily conserved across different organisms. However, differing subcellular localization is observed within these organisms. For example, MpfA, CorB, and CNNMs are localized to the plasma membrane, while plant MGR1/CST2 is localized to the tonoplast (Fig. 2b) (Tang *et al.*, 2022). These differences in subcellular localization suggest that they play different roles in $Mg^{2+}$ utilization in different organisms. Unlike animals, plants have developed vacuoles that occupy *c.* 90% of the cell volume and are exposed to varying $Mg^{2+}$ concentrations in soils from deficiency to excess levels, and sequestration of $Mg^{2+}$ into the vacuoles by MGR1/CST2 is therefore an important process in the maintenance of $Mg^{2+}$ homeostasis in the cytosol in plants.

Recently, several homologs of MGR1/CST2 have been functionally characterized in Arabidopsis. Unlike MGR1/CST2, MGR4-7 are localized at the plasma membrane of root xylem parenchyma cells and are involved in the xylem loading of $Mg^{2+}$ (Meng *et al.*, 2022). On the other hand, MGR8 and MGR9 are localized to the inner envelope of chloroplasts (Zhang *et al.*, 2022), where they are responsible for the uptake of $Mg^{2+}$. These findings indicate that MGR members have diverse roles in $Mg^{2+}$ transport and homeostasis. However, it remains to be examined in the future whether knockout of these MGR1/CST2 homologs also affects stomatal opening.

In summary, MGR1/CST2 expression in the guard cells is involved in stomatal opening in Arabidopsis. It functions to sequester $Mg^{2+}$ into the vacuoles, which is important for maintaining $Mg^{2+}$ homeostasis in guard cells and subsequently for stomatal opening, especially under high $Mg^{2+}$ conditions. Our work provides novel insights into the regulation of stomatal opening in fluctuating environments and highlights a novel role of MGR1/CST2 in plants.

## Author contributions

S-iI, T Kinoshita and JFM conceived and designed the experiments. S-iI, MH, KY, EG, SI, MO, SH, JFM and TS performed the experiments. S-iI, MH, KY, TS, T Kamura, T Kinoshita and

JFM analyzed the data. S-iI, T Kinoshita and JFM wrote the article.

## ORCID

Eiji Gotoh https://orcid.org/0000-0002-8952-987X
Maki Hayashi https://orcid.org/0000-0002-1704-8049
Sheng Huang https://orcid.org/0000-0002-2868-4331
Shuka Ikematsu https://orcid.org/0000-0002-4145-1380
Shin-ichiro Inoue https://orcid.org/0000-0003-4420-1106
Toshinori Kinoshita https://orcid.org/0000-0001-7621-1259
Jian Feng Ma https://orcid.org/0000-0003-3411-827X
Takamasa Suzuki https://orcid.org/0000-0002-1977-0510
Kengo Yokosho https://orcid.org/0000-0003-3935-268X

## Data availability

The data that support the findings of this study are available from the corresponding author upon reasonable request.

## References

Andrés Z, Pérez-Hormaeche J, Leidi EO, Schlücking K, Steinhorst L, McLachlan DH, Schumacher K, Hetherington AM, Kudla J, Cubero B *et al.* 2014. Control of vacuolar dynamics and regulation of stomatal aperture by tonoplast potassium uptake. *Proceedings of the National Academy of Sciences, USA* 111: E1806–E1814.

Arjona FJ, de Baaij JHF. 2018. CrossTalk opposing view: CNNM proteins are not $Na^+/Mg^{2+}$ exchangers but $Mg^{2+}$ transport regulators playing a central role in transepithelial $Mg^{2+}$ (re)absorption. *The Journal of Physiology* 596: 747–750.

Armitano J, Redder P, Guimarães VA, Linder P. 2016. An essential factor for high $Mg^{2+}$ tolerance of *Staphylococcus aureus*. *Frontiers in Microbiology* 7: 1888.

Assmann SM. 1988. Enhancement of the stomatal response to blue light by red light, reduced intercellular concentrations of $CO_2$, and low vapor pressure differences. *Plant Physiology* 87: 226–231.

de Carbonnel M, Davis P, Roelfsema MR, Inoue S, Schepens I, Lariguet P, Geisler M, Shimazaki K, Hangarter R, Fankhauser C. 2010. The Arabidopsis PHYTOCHROME KINASE SUBSTRATE2 protein is a phototropin signaling element that regulates leaf flattening and leaf positioning. *Plant Physiology* 152: 1391–1405.

Chen YS, Kozlov G, Moeller BE, Rohaim A, Fakih R, Roux B, Burke JE, Gehring K. 2021. Crystal structure of an archaeal CorB magnesium transporter. *Nature Communications* 12: 4028.

Chen ZC, Peng WT, Li J, Liao H. 2018. Functional dissection and transport mechanism of magnesium in plants. *Seminars in Cell & Developmental Biology* 74: 142–152.

Clough SJ, Bent AF. 1998. Floral dip: a simplified method for Agrobacterium-mediated transformation of *Arabidopsis thaliana*. *The Plant Journal* 16: 735–743.

De Angeli A, Zhang J, Meyer S, Martinoia E. 2013. AtALMT9 is a malate-activated vacuolar chloride channel required for stomatal opening in Arabidopsis. *Nature Communications* 4: 1804.

Doi M, Shigenaga A, Emi T, Kinoshita T, Shimazaki K. 2004. A transgene encoding a blue-light receptor, phot1, restores blue-light responses in the Arabidopsis *phot1 phot2* double mutant. *Journal of Experimental Botany* 55: 517–523.

Edgar RC. 2004. MUSCLE: multiple sequence alignment with high accuracy and high throughput. *Nucleic Acids Research* 32: 1792–1797.

Eisenach C, De Angeli A. 2017. Ion transport at the vacuole during stomatal movements. *Plant Physiology* 174: 520–530.

Flütsch S, Wang Y, Takemiya A, Vialet-Chabrand SRM, Klejchová M, Nigro A, Hills A, Lawson T, Blatt MR, Santelia D. 2020. Guard cell starch degradation

yields glucose for rapid stomatal opening in Arabidopsis. *Plant Cell* 32: 2325–2344.

Funato Y, Furutani K, Kurachi Y, Miki H. 2018. CrossTalk proposal: CNNM proteins are $Na^+/Mg^{2+}$ exchangers playing a central role in transepithelial $Mg^{2+}$ (re)absorption. *The Journal of Physiology* 596: 743–746.

Gibson MM, Bagga DA, Miller CG, Maguire ME. 1991. Magnesium transport in *Salmonella typhimurium*: the influence of new mutations conferring $Co^{2+}$ resistance on the CorA $Mg^{2+}$ transport system. *Molecular Microbiology* 5: 2753–2762.

Gotoh E, Oiwamoto K, Inoue SI, Shimazaki KI, Doi M. 2019. Stomatal response to blue light in crassulacean acid metabolism plants *Kalanchoe pinnata* and *Kalanchoe daigremontiana*. *Journal of Experimental Botany* 70: 1367–1374.

Guo FQ, Young J, Crawford NM. 2003. The nitrate transporter AtNRT1.1 (CHL1) functions in stomatal opening and contributes to drought susceptibility in Arabidopsis. *Plant Cell* 15: 107–117.

Hayashi M, Inoue SI, Ueno Y, Kinoshita T. 2017. A Raf-like protein kinase BHP mediates blue light-dependent stomatal opening. *Scientific Reports* 7: 45586.

Hayashi M, Sugimoto H, Takahashi H, Seki M, Shinozaki K, Sawasaki T, Kinoshita T, Inoue S. 2020. Raf-like kinases CBC1 and CBC2 negatively regulate stomatal opening by negatively regulating plasma membrane $H^+$-ATPase phosphorylation in *Arabidopsis*. *Photochemical & Photobiological Sciences* 19: 88–98.

Horrer D, Flütsch S, Pazmino D, Matthews JS, Thalmann M, Nigro A, Leonhardt N, Lawson T, Santelia D. 2016. Blue light induces a distinct starch degradation pathway in guard cells for stomatal opening. *Current Biology* 8: 362–370.

Huber SC, Maury W. 1980. Effects of magnesium on intact chloroplasts: I. Evidence for activation of (sodium) potassium/proton exchange across the chloroplast envelope. *Plant Physiology* 65: 350–354.

Inoue S, Iwashita N, Takahashi Y, Gotoh E, Okuma E, Hayashi M, Tabata R, Takemiya A, Murata Y, Doi M *et al.* 2017. Brassinosteroid involvement in *Arabidopsis thaliana* stomatal opening. *Plant & Cell Physiology* 58: 1048–1058.

Inoue S, Kaiserli E, Zhao X, Waksman T, Takemiya A, Okumura M, Takahashi H, Seki M, Shinozaki K, Endo Y *et al.* 2020. CIPK23 regulates blue light-dependent stomatal opening in *Arabidopsis thaliana*. *The Plant Journal* 104: 679–692.

Inoue S, Kinoshita T. 2017. Blue light regulation of stomatal opening and the plasma membrane $H^+$-ATPase. *Plant Physiology* 174: 531–538.

Inoue S, Kinoshita T, Matsumoto M, Nakayama KI, Doi M, Shimazaki K. 2008. Blue light-induced autophosphorylation of phototropin is a primary step for signaling. *Proceedings of the National Academy of Sciences, USA* 105: 5626–5631.

Inoue S, Takemiya A, Shimazaki K. 2010. Phototropin signaling and stomatal opening as a model case. *Current Opinion in Plant Biology* 13: 587–593.

Jossier M, Kroniewicz L, Dalmas F, Le Thiec D, Ephritikhine G, Thomine S, Barbier-Brygoo H, Vavasseur A, Filleur S, Leonhardt N. 2010. The Arabidopsis vacuolar anion transporter, AtCLCc, is involved in the regulation of stomatal movements and contributes to salt tolerance. *The Plant Journal* 64: 563–576.

Kinoshita T, Doi M, Suetsugu N, Kagawa T, Wada M, Shimazaki K. 2001. Phot1 and phot2 mediate blue light regulation of stomatal opening. *Nature* 414: 656–660.

Kumar S, Stecher G, Li M, Knyaz C, Tamura K. 2018. MEGAX: molecular evolutionary genetics analysis across computing platforms. *Molecular Biology and Evolution* 35: 1547–1549.

Kuromori T, Seo M, Shinozaki K. 2018. ABA transport and plant water stress responses. *Trends in Plant Science* 23: 513–522.

Lebaudy A, Hosy E, Simonneau T, Sentenac H, Thibaud JB, Dreyer I. 2008. Heteromeric $K^+$ channels in plants. *The Plant Journal* 54: 1076–1082.

Marten I, Deeken R, Hedrich R, Roelfsema MR. 2010. Light-induced modification of plant plasma membrane ion transport. *Plant Biology* 12: 64–79.

Martinoia E. 2018. Vacuolar transporters – companions on a longtime journey. *Plant Physiology* 176: 1384–1407.

Matthews J, Vialet-Chabrand S, Lawson T. 2020. Role of blue and red light in stomatal dynamic behaviour. *Journal of Experimental Botany* 71: 2253–2269.

Meng S-F, Zhang B, Tang R-J, Zheng X-J, Chen R, Liu C-G, Jing Y-P, Ge H-M, Zhang C, Chu Y-L *et al.* 2022. Four plasma membrane-localized MGR transporters mediate xylem Mg$^{2+}$ loading for root-to-shoot Mg$^{2+}$ translocation in *Arabidopsis*. *Molecular Plant* **15**: 805–819.

Mumberg D, Müller R, Funk M. 1995. Yeast vectors for the controlled expression of heterologous proteins in different genetic backgrounds. *Gene* **156**: 119–122.

Norén H, Svensson P, Andersson B. 2004. A convenient and versatile hydroponic cultivation system for *Arabidopsis thaliana*. *Physiologia Plantarum* **121**: 343–348.

Roelfsema MR, Hedrich R. 2005. In the light of stomatal opening: new insights into 'the Watergate'. *New Phytologist* **167**: 665–691.

Rusconi F, Simeoni F, Francia P, Cominelli E, Conti L, Riboni M, Simoni L, Martin CR, Tonelli C, Galbiati M. 2013. The *Arabidopsis thaliana MYB60* promoter provides a tool for the spatio-temporal control of gene expression in stomatal guard cells. *Journal of Experimental Botany* **64**: 3361–3371.

Santelia D, Lawson T. 2016. Rethinking guard cell metabolism. *Plant Physiology* **172**: 1371–1392.

Schroeder JI, Allen GJ, Hugouvieux V, Kwak JM, Waner D. 2001. Guard cell signal transduction. *Annual Review of Plant Physiology and Plant Molecular Biology* **52**: 627–658.

Shimazaki K, Doi M, Assmann SM, Kinoshita T. 2007. Light regulation of stomatal movement. *Annual Review of Plant Biology* **58**: 219–247.

Suetsugu N, Takami T, Ebisu Y, Watanabe H, Iiboshi C, Doi M, Shimazaki K. 2014. Guard cell chloroplasts are essential for blue light-dependent stomatal opening in Arabidopsis. *PLoS ONE* **9**: e108374.

Suzuki T, Kawai T, Takemura S, Nishiwaki M, Suzuki T, Nakamura K, Ishiguro S, Higashiyama T. 2018. Development of the Mitsucal computer system to identify causal mutation with a high-throughput sequencer. *Plant Reproduction* **31**: 117–128.

Tang RJ, Meng SF, Zheng XJ, Zhang B, Yang Y, Wang C, Fu AG, Zhao FG, Lan WZ, Luan S. 2022. Conserved mechanism for vacuolar magnesium sequestration in yeast and plant cells. *Nature Plants* **8**: 181–190.

Tominaga M, Kinoshita T, Shimazaki K. 2001. Guard-cell chloroplasts provide ATP required for H$^+$ pumping in the plasma membrane and stomatal opening. *Plant & Cell Physiology* **42**: 795–802.

Trachsel E, Redder P, Linder P, Armitano J. 2019. Genetic screens reveal novel major and minor players in magnesium homeostasis of *Staphylococcus aureus*. *PLoS Genetics* **15**: e1008336.

Uchida N, Lee JS, Horst RJ, Lai HH, Kajita R, Kakimoto T, Tasaka M, Torii KU. 2012. Regulation of inflorescence architecture by intertissue layer ligand-receptor communication between endodermis and phloem. *Proceedings of the National Academy of Sciences, USA* **109**: 6337–6342.

Ueno K, Kinoshita T, Inoue S, Emi T, Shimazaki K. 2005. Biochemical characterization of plasma membrane H$^+$-ATPase activation in guard cell protoplasts of *Arabidopsis thaliana* in response to blue light. *Plant & Cell Physiology* **46**: 955–963.

Willmer C, Fricker M. 1996. *Stomata*. London, UK: Springer Nature.

Wu W, Peters J, Berkowitz GA. 1991. Surface charge-mediated effects of Mg on K flux across the chloroplast envelope are associated with regulation of stromal pH and photosynthesis. *Plant Physiology* **97**: 580–587.

Yamaji N, Takemoto Y, Miyaji T, Mitani-Ueno N, Yoshida KT, Ma JF. 2017. Reducing phosphorus accumulation in rice grains with an impaired transporter in the node. *Nature* **541**: 92–95.

Yamazaki D, Funato Y, Miura J, Sato S, Toyosawa S, Furutani K, Kurachi Y, Omori Y, Furukawa T, Tsuda T *et al.* 2013. Basolateral Mg$^{2+}$ extrusion via CNNM4 mediates transcellular Mg$^{2+}$ transport across epithelia: a mouse model. *PLoS Genetics* **9**: e1003983.

Yang M, Jensen LT, Gardner AJ, Culotta VC. 2005. Manganese toxicity and *Saccharomyces cerevisiae* Mam3p, a member of the ACDP (ancient conserved domain protein) family. *The Biochemical Journal* **386**: 479–487.

Zeiger E, Hepler PK. 1977. Light and stomatal function: blue light stimulates swelling of guard cell protoplasts. *Science* **196**: 887–889.

Zhang B, Zhang C, Tang R, Zheng X, Zhao F, Fu A, Lan W, Luan S. 2022. Two magnesium transporters in the chloroplast inner envelope essential for thylakoid biogenesis in Arabidopsis. *New Phytologist*. doi: 10.1111/nph.18349.

Zhang H, Zhao FG, Tang RJ, Yu Y, Song J, Wang Y, Li L, Luan S. 2017. Two tonoplast MATE proteins function as turgor-regulating chloride channels in *Arabidopsis*. *Proceedings of the National Academy of Sciences, USA* **114**: E2036–E2045.

Zhao X, Qiao XR, Yuan J, Ma XF, Zhang X. 2012. Nitric oxide inhibits blue light-induced stomatal opening by regulating the K$^+$ influx in guard cells. *Plant Science* **184**: 29–35.

## Supporting Information

Additional Supporting Information may be found online in the Supporting Information section at the end of the article.

**Fig. S1** Gene mapping, structure and complementation test.

**Fig. S2** Effect of fusicoccin, an activator of plasma membrane H$^+$-ATPase on stomatal opening in the epidermis of wild-type and *cst2* mutants.

**Fig. S3** Structure and phylogenetic tree of MGR1/CST2.

**Fig. S4** Growth of wild-type and *cst2* mutants grown under different ionic stress conditions.

**Fig. S5** Growth and stomatal responses of *MGR1/CST2*-overexpressing plants.

**Table S1** Primers used in this study.

Please note: Wiley Blackwell are not responsible for the content or functionality of any Supporting Information supplied by the authors. Any queries (other than missing material) should be directed to the *New Phytologist* Central Office.